6 Photonic Device Technologies

6-1 Resonant type optical modulators for 10GHz band

Tetsuya KAWANISHI, Satoshi OIKAWA, Kaoru HIGUMA, Yoshiro MATSUO, and Masayuki IZUTSU

For band-type operations such as radio-on-fiber systems, effective optical modulation can be obtained by using resonant structures. In this paper, we propose a resonant-type optical modulator consisting of a simple planar structure, whose modulation efficiency is larger than that of conventional modulators. The normalized induced phase of the fabricated modulator has a peak of 3.41 at 10GHz, and the half wave voltage is 13.7V, while the length of the modulating electrode is 3.25mm.

Keywords
Optical modulator, Resonance, Impedance, Optical fiber, Radio communication

1 Introduction

In recent years, radio communication frequencies have become less available due to the popularization of mobile communications devices such as cellular phones and personal handyphone systems (PHS), and hence the necessity of exploiting frequency resources has intensified. As a solution, research has been conducted on radio-on-fiber systems that combine radio communication in millimeter wave bands and optical communication by means of optical fibers[1]. This communication system takes advantage of a large transmission loss in the millimeter wave band, whereby a single communication area is reduced, the same frequency is allocated to neighboring communication areas (to achieve more effective use of available radio communication frequencies), and point-to-point communication between base stations and the like is effected by converting radio signals into optical signals and transmitting them through broadband, low-loss optical fibers. Thus this communication system features both the benefits of radio communication (excellent distributivity and mobile capability) and of fiber-optic communication (broadband, low-loss communication). Communication systems such as this one have already been applied not only to outdoor communication devices such as the cellular phone but also to indoor communications systems, such as for wireless LANs.

In the radio-on-fiber system mentioned above, the optical modulator is required to be compact and to feature high efficiency. However, since many optical communication systems use digital modulation, the optical modulators are required to feature broadband optical response, which runs counter to the requirements of the radio-on-fiber system. To respond to these particular requirements, we have developed a resonant-type optical modulator that is compact and achieves high modulation efficiency through the use of electric resonance. As an initial step, we reported on a resonant optical modulator capable of operating in the 60-GHz band[2][3]. A modulating electrode with an open end was used with a

length of around λ/2; high-efficiency modulation was performed by setting a standing wave on the electrode. Note that when the length of the modulating electrode is set to λ/2, the voltage amplitude on the modulating electrode cannot be increased, because the impedance in terms of the feeding point becomes low. To circumvent this problem, a modulator was added with an impedance-matching circuit to enable the matching impedance in terms of the feeder electrode to have a modulation frequency of 50Ω. In our initial proposal, this impedance-matching circuit was specified to use patch-type capacitance, with which highly efficient modulation was to be performed. However, since a number of films need to be formed with patch-type capacitance, this proposal presented a problem in that, as the total number of fabricating procedures increases, characteristics may fluctuate because of the circuit's three-dimensional structure.

To address these problems, we have proposed a structure whereby the impedance-matching circuit is improved, replacing patch-type capacitance with stubs with a planar structure[4]. This stub structure has several merits: the stubs can be formed at one time with the formation of the modulating electrode, and thus additional fabricating procedures are not necessary; fluctuations in characteristics are small due to the planar structure; further, any fluctuations may be mitigated by trimming the stubs; and so on. However, the stubs present additional problems, such as enlargement of the optical modulator due to the addition of stubs on the opposite side of the feeder electrode and the deterioration of modulation efficiency due to the modulating electrodes featuring a CPW structure, to name two such problems.

Here we have proposed a resonant-type optical modulator with a planar structure, which solves the problems of the previous stub electrodes and which is compact and features high modulation efficiency. Moreover, in addition to this change in the structure, we have re-examined our design method in light of the requirement that the impedance be matched to 50Ω at the modulation frequency, producing an original design as a result [5][6][7]; we also report on the results of a prototype fabricated based on this design.

2 Circuit configuration and induced phase

An outline drawing of the optical modulator proposed here is shown in Figs.1 and 2. The optical modulator is composed of a Mach Zehnder (MZ) optical waveguide and electrodes on a z-cut $LiNbO_3$ substrate. The electrodes are comprised of a modulating electrode and the stubs. The modulating electrode is an electrode facilitating interaction with light and features an ACPW (Asymmetric CPW, or Asymmetric Coplanar Waveguide) structure to enhance modulation efficiency. This configuration has several merits: conductor loss is low and the electric field efficiency of the optical waveguide is high relative to a CPW structure, thus providing higher modulation efficiency than that afforded by a CPW structure. Further, the stubs are composed so as to generate parallel resonance with the modulating electrode, and each stub is extended obliquely from a junction of the feeder electrode and the modulating electrode.

The adoption of this configuration for the modulating electrode and the stubs solves the problem that arises with patch-type capacitors with a three-dimensional structure, as a planar circuit is employed instead; the configuration

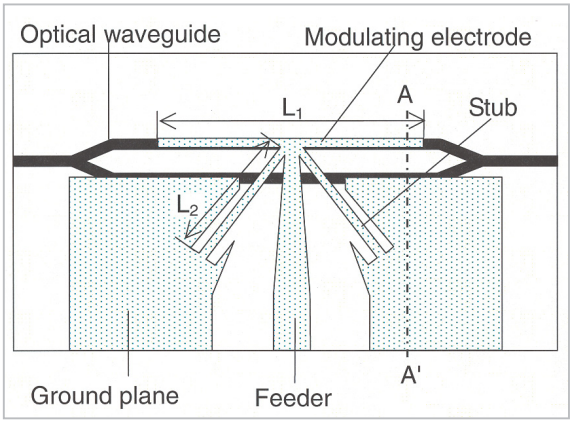

Fig.1 *Structure of a resonant-type modulator (top view)*

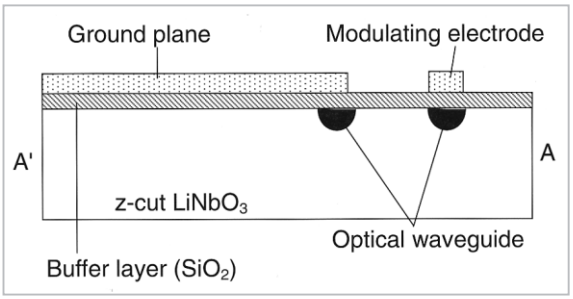

Fig.2 *Cross section of A-A´ (cross-sectional view)*

also solves the problems presented by optical modulators that employ conventional stubs, through placement of the stubs on the feeder electrode side.

An equivalent circuit for the optical modulator proposed here is shown in Fig.3. The termination impedance of the modulating electrode is expressed by Zt, so that this equivalent circuit can be applied to a modulating electrode with an open end and one with a short end. In the case of an open-ended modulating electrode, Zt becomes ∞; in the case of a short-ended modulating electrode, Zt becomes 0.

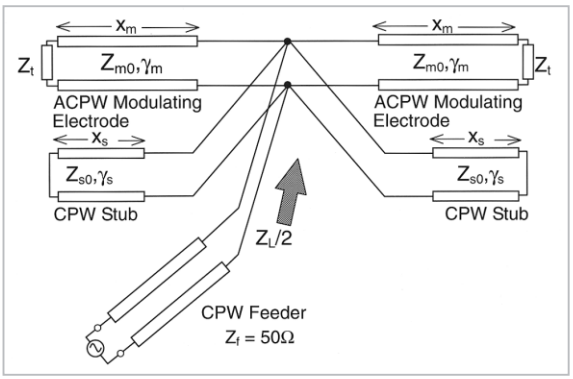

Fig.3 *Equivalent circuit for an optical modulator*

The characteristics of this optical modulator are then calculated using the equivalent circuit shown in Fig.2. Since the feeder electrode is connected to the center of the resonant electrode, the modulating electrode and the stubs are symmetrically configured in relation to the feeding point. First, the impedance Z_L of a parallel circuit consisting of a portion of the modulating electrode and the stub electrode on one side is obtained as

$$Z_L = \begin{cases} \dfrac{Z_{m0}Z_{s0}\coth\gamma_1 x_m \tanh\gamma_2 x_s}{Z_{m0}\coth\gamma_1 x_m + Z_{s0}\tanh\gamma_2 x_s} & (Z_t=\infty)\cdots(1) \\ \dfrac{Z_{m0}Z_{s0}\tanh\gamma_1 x_m \tanh\gamma_2 x_s}{Z_{m0}\coth\gamma_1 x_m + Z_{s0}\tanh\gamma_2 x_s} & (Z_t=0)\cdots(2) \end{cases}$$

where Z_{m0}, γ_m, and x_m denote the characteristic impedance, the propagation constant, and the length of the modulating electrode, respectively, and similarly Z_{s0} γ_S, and x_s denote the corresponding parameters of the stub electrode, respectively. Since the synthetic impedance of two pairs of the modulating electrode and the stub electrodes at the feeding point becomes $Z_L/2$ (refer to the arrow in Fig.3), the voltage transmissivity T at the feeding point can be expressed by the following expression:

$$T = \frac{2Z_L}{Z_L + 2Z_f} \qquad \cdots(3)$$

where Z_f is the characteristic impedance (50 Ω) of the feeder electrode.

Denoting the modulation frequency by f and the input voltage from the feeder electrode by V_{in}, the voltage at a distance x from the feeding point on the modulating electrode by is given by

$$V(x,t)=\mathrm{Re}[TF(x)e^{j2\pi ft}] \qquad \cdots(4)$$
$$V(x,t)=V_{in}V(x,t)$$

Here, $F(x)$ represents the voltage distribution on the modulating electrode and is defined as

$$F(x) \equiv \begin{cases} \dfrac{\cosh\gamma_m(x_m-x)}{\cosh\gamma_m x_m} & (Z_t=\infty) \qquad \cdots(5) \\ \dfrac{\sinh\gamma_m(x_m-x)}{\sinh\gamma_m x_m} & (Z_t=0) \qquad \cdots(6) \end{cases}$$

Since the phase change induced in each optical waveguide is represented by the sum total of the electro-optic effect seen from a coordinate system that moves at the propagation speed of light, the phase difference (induced phase) ϕ induced between the two optical waveguides of the MZ structure is given by the following expression:

$$\phi = \frac{\pi}{\lambda} n_o^3 r_{33} (\Gamma_2 - \Gamma_1) L_1 \frac{V_{in}}{s} \frac{1}{L_1} \int_{-x_m}^{x_m} V(|x|, \frac{x}{c} n_o + t) dx$$
$$= \frac{\pi}{\lambda} n_o^3 r_{33} (\Gamma_2 - \Gamma_1) L_1 \frac{V_{in}}{s} \Phi \cos(2\pi f t + \varphi) \quad \cdots (7)$$

Here, s is the electrode spacing of the modulating electrode, r_{33} is the Pockels coefficient (30.8×10^{-12}m/V)[8], λ is the light wavelength, $L_1 \equiv 2x_m$ is the length of the modulating electrode, and n_o is the refractive index of the optical waveguides. Γ_1 and Γ_2 are the electric-field reduction coefficients, each of which shows an overlap between the electric field of the light and the electric field of the modulating electrode; TEM approximate analysis produces a calculated value of $\Gamma_2 - \Gamma_1$ = 1.318. Further, Φ corresponds to the phase induced as a function of the unit length; it is referred to here as the "normalized induced phase." This normalized induced phase becomes unity for a traveling-wave optical modulator with lossless electrodes in which the velocity is completely matched. Since the loss is present in the actual electrodes, the normalized induced phase always becomes a value less than unity in a traveling-wave optical modulator. In a resonant-type optical modulator, this normalized induced phase may take on a value larger than unity due to the voltage increase of the resonant circuit and hence can be considered to represent a degree of modulation efficiency.

3 Design method

With a conventional design (where impedance in relation to the feeder electrode is matched to 50 Ω at the modulation frequency), the length of the modulation electrode and the electrostatic capacity of the patch-type capacitance, or the length of the stubs, are varied. With this prototype, designed to maximize the normalized induced phase, we varied the lengths of the modulating electrode and the stubs.

The optical modulator is based on the operating principle that modulation efficiency is enhanced by generating large voltage amplitudes on the modulating electrode. For this purpose, the modulating electrode and the stubs are adjusted to resonate parallel so that the impedance is increased at the feeding point, thereby increasing the voltage transmission coefficient. The design procedure based on this operating principle is as follows.

1) To adapt the modulator to the modulation frequency, the film thicknesses of the buffer layer and of the electrode and the structure of the stub (either open-ended or short-ended) are specified.
2) The impedances of the modulating electrode and of the stubs and the propagation constant at the modulation frequency are calculated by an electromagnetic field simulator.
3) Using the impedances and the propagation constant thus calculated in 2), the optimal length of electrode to maximize normalized induced phase Φ is determined.

Here we will describe a sample design for a modulation frequency of 10 GHz attained using this procedure. For the electromagnetic field simulator, the HFSS (Ver. 5.4) from Agilent Technologies was used.

The composition of the optical modulator is shown in Fig.1. The modulator was composed of a buffer layer with a thickness of 0.55 μm; the electrode thickness was 2 μm. The end of the modulating electrode was set to be open-ended (Z_t=∞), the width of the central conductor was set at 5 μm, and the gap of the electrodes was set at 27 μm. With these specifications, the characteristic impedance Z_{m0} and the propagation constant γ_m at 10 GHz were calculated to be Z_{m0} = 66.6 Ω and γ_m = 27.8 + j740.6, respectively. Each stub was short-ended, and the width of the central conductor and the gap of the electrodes were set at 50 μm and 27 μm, respectively. The central conductors were set wider than the modulating electrode for purposes of reducing electrode loss. The characteristic impedance Z_{s0} and the propagation constant of the stubs γ_s at a frequency of 10 GHz were calculated to be Z_{s0} = 26.5 Ω and γ_s = 17.64 + j882.3, respectively.

Using these values, the length of the modulating electrode x_m and the length of the stubs x_s at which the normalized induced phase Φ

became the maximum were derived using calculations with variable values of x_m and x_s. As a result, the phase was maximized with a combination of $x_m = 0.19\lambda_m$, and $x_s = 0.12\lambda_s$ (λ_m and λ_s are the wavelengths on the modulating electrode and on the stub electrodes, respectively). The voltage distribution (modulation frequency: 10 GHz) on the modulating electrode in this case is shown in Fig.4. A voltage distribution without the stubs is also shown to confirm the effect of the stubs electrodes. With the stubs, a larger voltage is generated on the whole electrode, and therefore the effectiveness of the stub structure can be confirmed. Further, the impedance in relation to the feeding point and reflectivity as a function of frequency both with the stubs and without the stubs is shown in Fig.5. In the vicinity of 10 GHz (the modulation frequency) with the stubs, the reflectivity was small and the impedance reached the relative maximum; without the stubs, the reflectivity was not less than 0.9 and the impedance was also small. From these results, the effect of the stubs has been confirmed.

Frequency response of the normalized induced phase is shown in Fig.6. The normalized induced phase reaches its relative maximum at 10 GHz and the value is 2.34. Comparing these results with those of the traveling-wave optical modulator whose normalized

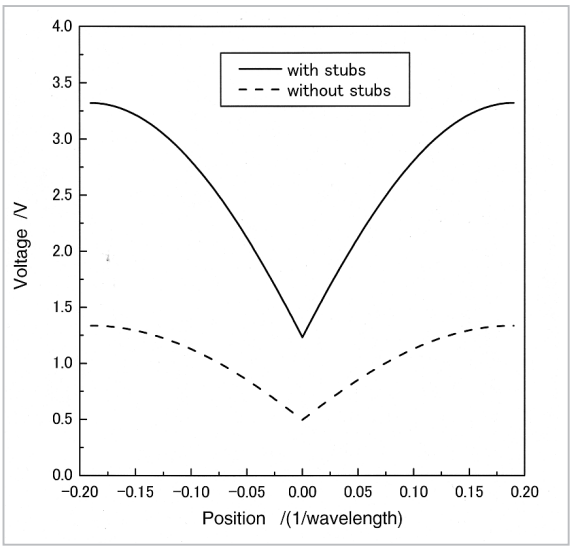

Fig.4 *Distribution of voltage on electrode*

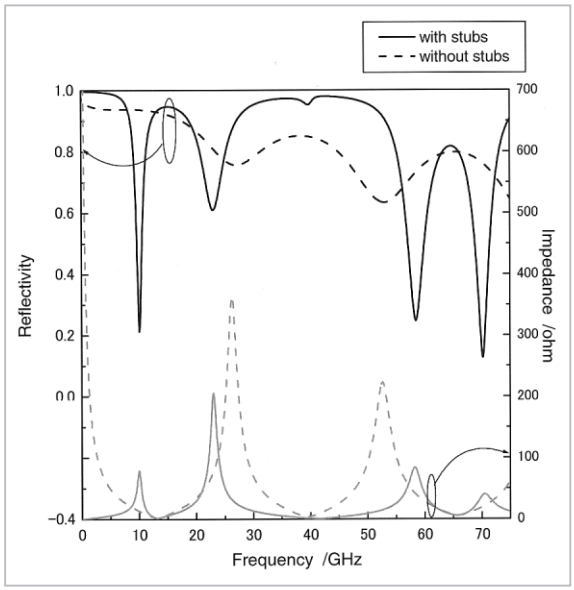

Fig.5 *Reflectivity*

induced phase did not exceed unity, it was found that modulation efficiency was increased by a factor of 2.0 or more. An electric field distribution was calculated using the 3-D finite element method (HFSS Ver. 5.4). As shown in Fig.7, taking advantage of the symmetric property of the structure, analysis was performed in half of the region. The electric field distribution obtained is shown in Fig. 8. It can thus be confirmed that a large electric field is generated in the resonant electrode.

Moreover, a half-wave voltage $V\pi$, at which the phase difference between two optical waveguides becomes π, can be calculated with the expression (8), which yields 12.2 V as a design value. Here, the wavelength of the light is assumed to be 1.55 μm.

$$V_\pi = \frac{\lambda s}{n_o^3 r_{33}(\Gamma_2 - \Gamma_1) L_1 \Phi} \qquad \cdots(8)$$

4 Prototype results

Based on the design discussed in the previous section, a prototype of the optical modulator was fabricated and evaluated. The length of the modulating electrode L_1 and the length of the stubs L_2 were determined to be $L_1(= 2\times x_m) = 3.250$ mm and $L_2(= x_s) = 0.875$ mm, respectively, based on the lengths of the elec-

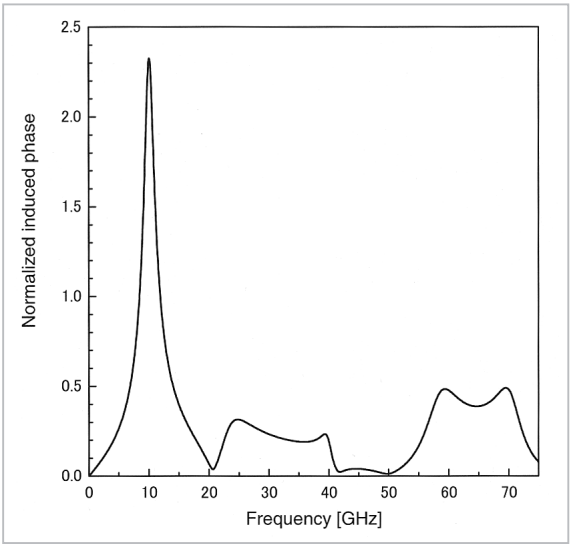

Fig.6 *Frequency response of normalized induced phase*

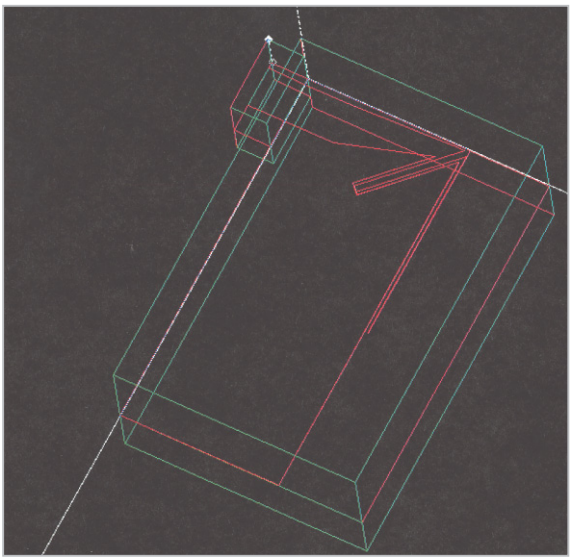

Fig.7 *Structural model of a resonant-type modulator used in calculating electric field distribution*

trodes $x_m = 0.19\,\lambda_m$ and $x_s = 0.12\,\lambda_s$ at which Φ becomes the maximum and the design values of the propagation constants γ_m and γ_s. When comparing the prototype with a traveling-wave optical modulator, where the shortest electrode length is 20 mm, it can be seen that the proposed modulator is extremely compact.

The frequency responses of the normalized induced phase as designed and as measured are shown in Fig.9. The measured values exhibit a peak of 2.65 at 10.8 GHz. Although a dip was seen at about 11 GHz in the measured values, in terms of frequency response,

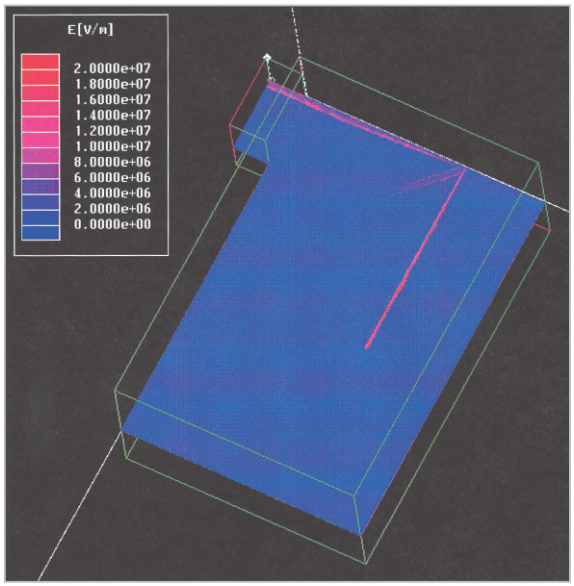

Fig.8 *Simulated electric field distribution on resonant electrode*

the measured values demonstrated excellent agreement with the design values. It is thought that the variation in peak frequency was caused by differences in the propagation constant and in the impedance value between the design and the prototype.

Incidentally, for $V\pi$ at the peak frequency, the measured value was 17.1 V. The deviation of measured $V\pi$ from the design value (12.2V) is attributed to the fact that the electric-field reduction coefficient calculated by TEM approximate analysis deviates in practice due to the influence of variations in the thickness-

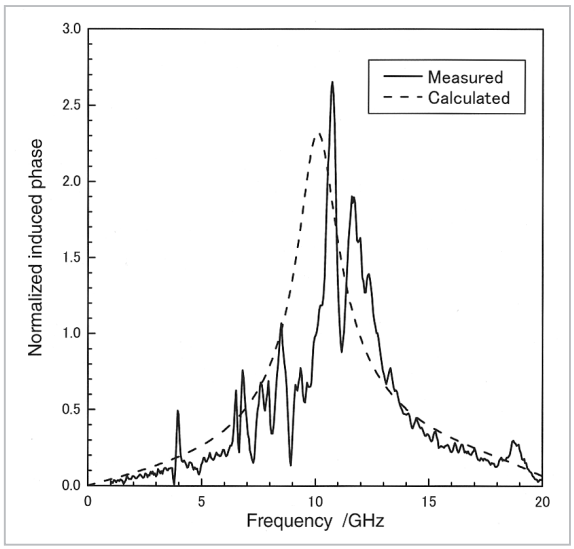

Fig.9 *Comparison between design values and prototype results*

es of the buffered layer and of the electrode.

In light of the potential differences between the design and actual values (such as the value of the propagation constant), the lengths of the modulating electrode and of the stub electrodes were varied from the design values within ranges of ± 5% and ± 10%, respectively, the prototype thus fabricated was then evaluated. The evaluation results are summarized in Table 1. Table 1 shows results for a prototype whose stub electrodes were extended by 10%, ϕ where $V\pi$ reached maximums of 3.41 and 13.7 V, respectively; the peak frequency was shifted to 10.6 GHz. It is thought that the deviation of ϕ from the design value to a higher value may be attributed to the influence of variations in the propagation constant and in the impedance, as with the variation of the peak frequency. However, the difference between the design value and the measured value of the peak frequency was not large, and in terms of the frequency response of the normalized induced phase, the design values and the measured values demonstrated excellent agreement. From the foregoing results, the effectiveness of this design was confirmed at a modulation frequency of 10 GHz.

Table 1 *Peak frequency, half-wave voltage, and normalized induced phase with variation in the length of the electrodes*

L_1 [%]	L_2 [%]	Peak Frequency [GHz]	Vπ [V]	φ
100	100	10.8	17.1	2.65
90	100	12.5	17.2	2.92
95	100	10.4	18.8	2.61
105	100	10.4	16.9	2.63
110	100	10.6	15.6	2.64
100	90	12.5	25.0	1.81
100	95	10.5	17.2	2.69
100	105	10.7	15.5	2.98
100	110	10.6	13.7	3.41

5 Conclusion

In this study, a resonant-type optical modulator featuring higher modulation efficiency than conventional optical modulators and a compact, simple planar structure was investigated. Based on a method of calculating the combination of electrode characteristics that will maximize normalized induced phase, an optimal modulating electrode length of 3.250 mm and a stub length of 0.875 mm were determined for a modulation frequency of 10 GHz. Evaluation of a trial optical modulator revealed that the frequency response of the actual normalized induced phase demonstrated excellent agreement with the design values. Further, the optical modulator has been demonstrated to be compact and to feature high modulation efficiency (such as a normalized induced phase of 3.41 at the peak). In the future, we intend to design and produce a prototype of a modulator featuring a modulation frequency other than 10 GHz, to confirm the effectiveness of this design method at even higher frequencies.

References

1 H.Ogawa, Microwave and Millimeter-wave fiber optic technologies for subcarrier transmission systems, IEICE Trans. On Comm.,E76-B,1078-1090 (1993).

2 S. Oikawa, S.Shimotsu, T.Saito, M.Sasaki, T.Kawanishi, M.Izutsu, "60GHz resonant-type $LiNbO_3$ optical modulator", Sumitomo Osaka Cement Technical Report,pp14-17(2000).

3 M.Sasaki, D.Dawn, T.Kawanishi, S.Shimotsu, S. Oikawa, M.Izutsu, "60GHz resonant-type $LiNbO_3$ optical modulator", IEICE general conference,C-3-125(1999).

4 S.Oikawa, T.Miyazaki, T.Kawanishi, M.Izutsu, "10GHz resonant-type $LiNbO_3$ optical modulator", IEICE general conference,C-3-15(2000).

5 T.Kawanishi, S.Oikawa, M.Izutsu, "Resonant-type optical modulator with planer structure", Technical report of IEICE, LQE2001-3(2001).

6 T. Kawanishi, S. Oikawa, K. Higuma, Y. Matsuo and M. Izutsu, $LiNbO_3$ resonant-type optical modulator with double-stub structure, Electron. Lett. 37, 1244-1246 (2001).

7 T. Kawanishi, S. Oikawa, K. Higuma, M. Sasaki and M. Izutsu, Design of $LiNbO_3$ optical modulator with an asymmetric resonant structure, IEICE Trans. Electron E85-C, 150-155 (2002).

8 H.Nishihara, M.Haruna, T.Suhara, Optical integreted circuit, Ohmsha

***Tetsuya KAWANISHI**, Ph. D.*

Senior Researcher, Photonic Information Technology Group, Basic and Advanced Research Division

High-speed Lightwave modulation

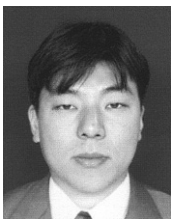

Satoshi OIKAWA

Guest Researcher, Photonic Information Technology Group, Basic and Advanced Research Division

High-speed Lightwave modulation

Kaoru HIGUMA

Guest Researcher, Photonic Information Technology Group, Basic and Advanced Research Division

High-speed Lightwave modulation

***Yoshiro MATSUO**, Ph. D.*

Research Fellow, Photonic Information Technology Group, Basic and Advanced Research Division

High-speed Lightwave modulation

***Masayuki IZUTSU**, Dr. Eng.*

Distinguished Researcher

Opt-Electronics